AR-009-365

DSTO-TR-0234

A Practical Utilisation of Middleton
EMI Models: Automated Modelling,
Parameter Estimation and
Optimisation

M.S. Britton and M.L. Scholz

1996 0212 218

D E P A R T M E N T ◆ O F D E F E N C E

DEFENCE SCIENCE AND TECHNOLOGY ORGANISATION

A Practical Utilisation of Middleton EMI Models: Automated Modelling, Parameter Estimation and Optimisation

M. S. Britton & M. L. Scholz

ABSTRACT

A procedure is proposed for analysing electromagnetic interference (EMI) with Middleton models. An introduction to the models is given, and descriptions of automated procedures for estimation and optimisation of model parameters are proposed. Various techniques are developed to solve numerical problems in the calculation of the model parameters. Many of the practical problems associated in the analysis are outlined.

RELEASE LIMITATION

Approved for public release

DTIC QUALITY INSPECTED 4

APPROVED FOR PUBLIC RELEASE

A Practical Utilisation of Middleton EMI Models: Automated Modelling, Parameter Estimation and Optimisation

EXECUTIVE SUMMARY

This report presents the results of an analysis of high-frequency electromagnetic interference (HF EMI or 'radio noise'). The aim of the analysis was to develop software to model HF EMI and extract useful physical information from those models as a basis for simulation. Sections concerning data acquisition and processing are present.

The software successfully modelled the HF EMI using Middleton's models. However, the extraction of useful physical information was limited, as the models are quite complex and information available in the literature is incomplete. The modelling procedures nevertheless provide a useful insight into HF EMI and could form the basis for modem performance simulation tests, using information about interferer positions, densities, transmitting powers, etc. That is, interference would be simulated entirely by approximate physical situations, compared with traditional methods using physically meaningless parameters.

THIS PAGE IS INTENTIONALLY BLANK

Authors

Matthew S. Britton
Communications Division

Completed B. Eng (Electronic Engineering) at the University of South Australia in 1994. He is currently employed in the Network Architectures discipline as a professional officer (PO1). Matthew has undertaken research into analysis, modelling and simulation of HF radio noise, and is currently involved in performance studies of communications network protocols.

Marcel L. Scholz
Communications Division

Completed B. App. Sc (Physics) at the University of Adelaide in 1972 and Grad. Dip in Operations Research at the University of South Australia in 1984. Marcel's previous work at DSTO has been in the fields of applied laser physics, operational research and combat systems integration. He is currently employed in the Network Architectures discipline as a senior scientist (SPOB) conducting simulation and related research into HF radio noise and the performance of military communications protocols in wide area networks.

THIS PAGE IS INTENTIONALLY BLANK

Contents

Figures

THIS PAGE IS INTENTIONALLY BLANK

1   Introduction

Middleton's EMI models aim to provide realistic, quantitative descriptions of man-made and natural EMI environments, accurate even with highly non-Gaussian random processes. All model parameters can be extracted from measurement, are physically meaningful, and the model's structures are based on underlying physics of radio wave propagation and reception. Hence knowledge of the model's parameters provides insight as to the physical processes taking place. What this in effect means is that the EMI process resulting from the sources incident on the receiver may be simulated with the knowledge of several key parameters.

The authors aim firstly to impart a basic knowledge of the Middleton EMI models (omitting the mathematical derivations) and to explain in exactly what way its parameters are physically meaningful. Methods are then proposed to enable extraction of estimates of model parameters from data samples, and to optimise these parameters. The question "How well does the model fit the empirical data" is answered. Many of the numerical problems and solutions associated with such a process are given, however, details of the actual computer algorithm structures are omitted. The paper also explains in simple terms how the algorithms decide on which model (Class A or B) to use, and how this affects the estimation and optimisation routines.

There are several other non-Gaussian EMI models that may be of use. The Kabanov [13, pp, 122–129] and K-distributed [14] models have shown promise: what may be considered a flaw in these two models is their lack of insight into the physical mechanisms behind the EMI. It is for this reason that Middleton models are favoured for analysis.

2   The Middleton EMI Models

2.1   General Description

There are three classes of Middleton models: A, B, and C. Class A models are used when the noise bandwidth is narrower than the receiver bandwidth, producing ignorable transients in the receiver's front-end RF and IF (radio and intermediate frequency respectively) stages. Class B models are used when the incoming noise is spectrally wider than the receiver bandwidth, so that transient effects in build up and delay occur to produce 'ringing.' Class C EMI may occur when both Class A and B interferers are present. However, as information available on Class C models is severely limited, comments concerning them shall not occur again in this discussion.

The Middleton models are supposedly effective for naturally occurring or man-made noise processes (occurring separately or simultaneously) for signals containing intelligent or random components. They fail when the data samples are either (i) nonstationary[1], or (ii) inhomogeneous.

---

[1]In the context of this paper, stationarity is assumed to be present if the underlying probabilistic mechanisms are time-invariant during the data acquisition period. For example, there are no changes in average emitter numbers, propagation laws, emitter locations, etc. A change in this mechanism during

Worthy of note is the fact that the models assume incident signal phases to be uniformly distributed on $[0, 2\pi]$. With multipath effects, this may not be the case. Also, the models assume two independent components: (i), Poisson-distributed (in space and time) 'impulsive' EMI, containing only a few (ten or less) discrete sources of relatively high level, and (ii), zero-mean Gaussian background noise from either receiver (self-generated) noise or external noise. There are five more assumptions regarding the physical processes of source emissions; however these may prove less crucial (refer [3, p.8.]) They are; (a) a far-field (Fraunhofer) condition exists [8]; (b) there is little relative motion (viz. Doppler shift) between sources and receiver; (c) the typical source has a beam pattern that is not necessarily omni-directional; (d) the receiving antenna generally has a directional beam pattern; and (e) the source may have a time-variable probabalistic mechanism (e.g., change in level, frequency).

Because of the form of the EMI, it becomes useful to graphically represent the data on what is called a Rayleigh Probability Presentation (RPP), which is basically a log-log by log scale (specifically, it is a $log_{10}[-ln[...]]$ vs $log_{10}[...]$ scale) plot. The RPP shows many characteristics of the signal's envelope, including the percentage of time it is Rayleigh-behaved (as is thermal noise). Thermal (Gaussian, or Rayleigh-enveloped) noise appears as a straight line with gradient $-\frac{1}{2}$ on a RPP. The vertical axis displays the quotient of the envelope voltage E and the root mean square of the envelope voltage E_{rms}, while the horizontal axis displays the percentage of time a certain envelope threshold E_o is exceeded, and is hence referred to as 'exceedance probability'. The plot is therefore known as an Amplitude Probability Distribution (APD).

2.2   The Middleton Class B EMI model

Figure 1 shows a typical APD for Class B EMI. Shown clearly are two regions, BI and BII, separated by an *inflection point* IP. ϵ and ϵ_0 are the normalised envelope voltage and the corresponding threshold respectively. The composite model may be considered an approximation for low and high values of the envelope. Region I, which is an approximation for low envelope values is described by the equation:

$$P_{BI}[\epsilon > \epsilon_0] = 1 - \hat{\epsilon_0}^2 \times \sum_{n=0}^{\infty} \frac{(-1)^n \times \hat{A}_{\alpha}^n \times \Gamma(1 + \frac{\alpha n}{2}) \times M(1 + \frac{\alpha n}{2}; 2; -\hat{\epsilon_0}^2)}{n!}, \quad \epsilon_0 < \epsilon_B \quad (1)$$

where:

$$\hat{A}_{\alpha} = \frac{A_{\alpha}}{(2 \times G)^{\alpha}},$$

$$G = \sqrt{(\frac{4 - \alpha}{2 - \alpha} + \Phi_B)(\frac{1}{4(1 + \Phi_B)})},$$

data-acquisition would be reflected by a changing APD and hence changing model parameters.
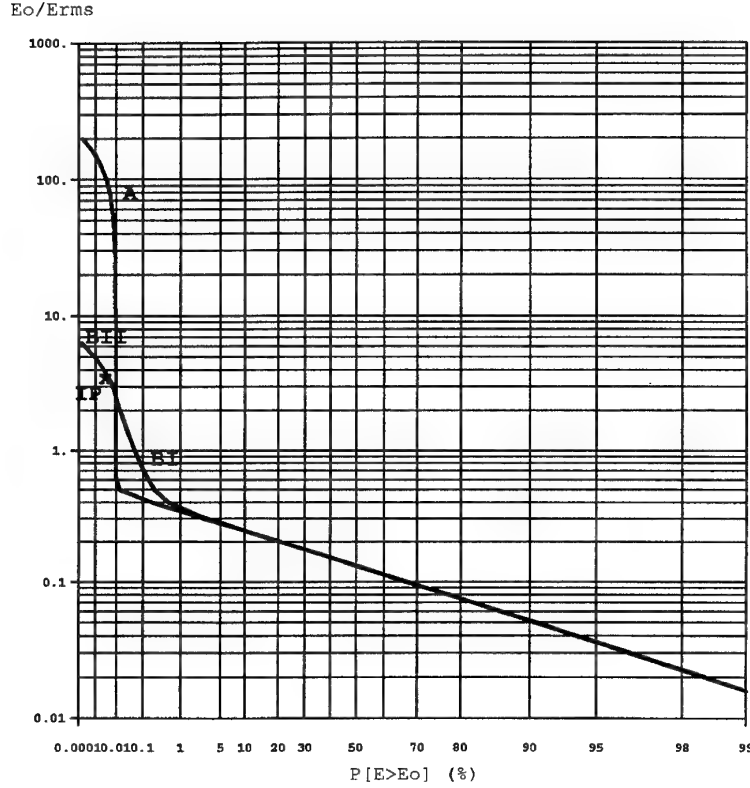
Eo/Erms

Figure 1: Typical models (Class B model parameters: α=1.8, Ω_B=0.47, Φ_B=5, N_I=1.63, A_α=1, A_B=0.0001, Class A model parameters: A_A=0.001, Ω_A=1, Φ_A=1)

$$\hat{\epsilon_0} = (\frac{\epsilon_0 \times N_I}{2 \times G}),$$

and $\epsilon_0 = \dfrac{E_0}{\sqrt{2 \times \Omega_B \times (1 + \Phi_B)}} \equiv$ normalised envelope threshold

α	$\equiv$	spatial density propagation parameter
Ω_B	$\equiv$	intensity of the impulsive component
Φ_B	$\equiv$	ratio of the intensities of the Gaussian to the non-Gaussian components
E_0	$\equiv$	un-normalised envelope threshold
N_I	$\equiv$	scaling parameter
Γ	$\equiv$	Gamma function
M	$\equiv$	Kummer's confluent hypergeometric function
A_α	$\equiv$	scaling parameter

Region I has a finite non-zero gradient on the APD at low probabilities, and as such

does not satisfy the condition for finite energy (and hence the existence of all finite moments of the envelope.) The required 'bend-over', provided by Region II, has the form:

$$P_{BII}[\epsilon > \epsilon_0] = e^{-A_B} \times \sum_{m=0}^{\infty} \frac{A_B^m \times \text{Exp}[\frac{-\epsilon_0^2}{\sigma_B}]}{m!}, \quad \epsilon_0 > \epsilon_B \tag{2}$$

where:

$$\sigma_B = \frac{(\Phi_B + \frac{m}{\hat{A}_B})}{(1 + \Phi_B)},$$

$$\hat{A}_B = A_B \times (\frac{2 - \alpha}{4 - \alpha}),$$

and $A_B \equiv$ impulsive index

2.3   The Middleton Class A EMI model

Class A models are relatively more straight-forward to derive than Class B models[2]. Visually, it is simple to distinguish between the two on an APD, Class A having a more pronounced 'elbow' region than Class B. An example is shown in Figure 1. It is not a composite model: the one equation describing it being;

$$P_A[\epsilon > \epsilon_0] = e^{-A_A} \sum_{m=0}^{\infty} \frac{A_A^m \times \text{Exp}[\frac{-\epsilon_0^2}{\sigma_A}]}{m!}, \tag{3}$$

where:

$$\sigma_A = \frac{(\Phi_A + \frac{m}{A_A})}{(1 + \Phi_A)},$$

where Φ_A and A_A are analogous to their respective Class B parameters.

Class B models will usually work well with atmospheric and ignition noise, etc., while (in general) Class A will work with 'intelligent' (that is, man-made narrowband EMI meant to convey information—eg, modems.) noise processes. This depends on the receiver bandwidth, which is usually assumed wider than narrow-band intelligent EMI.

---

[2]A point worth noting is that Class A EMI is a special case of (Region II) Class B EMI, as $\alpha \to \infty$.

2.4   Physical Significance of Model Parameters

The physical meaning of these parameters may now be given, beginning with Region I in the Class B model. $\Phi_{A,B}$ is the ratio of the intensities of the Gaussian to the non-Gaussian components[3]; on the APD it is the $Eo/Erms$ value where the data begins to depart from Rayleigh (straight-line) behaviour. The actual values of the above intensities given above may be found quite easily, by methods explained below. Another parameter, $\Omega_{A,B}$, that is not shown above but is used in the process, is the intensity of the impulsive component. The mean-square envelope of the resultant signal can be calculated by using the above two (shape) parameters:

$$\overline{E^2} = 2\Omega_{A,B}(1 + \Phi_{A,B})$$

$A_{A,B}$ is the impulsive index: the product of the average number of source emission events detected by the receiver and the mean duration of a typical intefering source emission. Very large values indicate a high density of overlapping waveforms at a given instant, giving an (asymptotically) Gaussian form to the EMI, as is shown in Figure 2(a). Low values indicate little overlapping, and hence the contributions of only a few sources are significant at a given instant, as is shown in Figure 2(b). This case would imply a highly impulsive resultant waveform. Graphically, $A_{A,B}$ is the exceedance probability value where the inflection occurs, and as such this property of the signal may be easily seen at a glance.

α $(0 \leq \alpha \leq 2)$ is the spatial density propagation parameter, since its value depends on the interacting spatial effects of source density and source propagation. That is, the effective source density and the propagation law (signal attenuation with distance) are both functions of α. Graphically, it is a complex measure of the gradient of the empirical APD in a small interval below the inflection point. Point A is used as a source in this example, and is d units from the receiver. α allows the following to be said about the receiver power P_R:
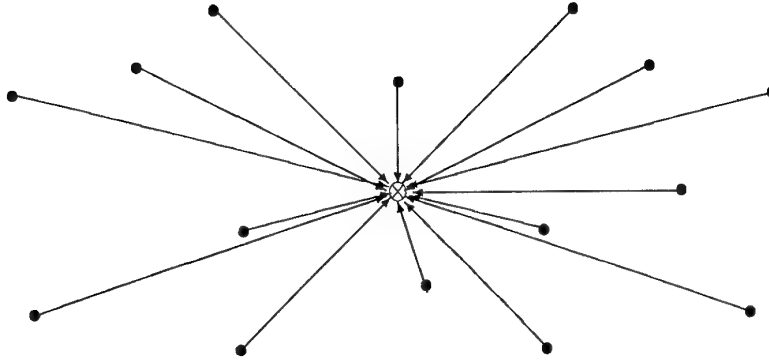
$$P_R \propto \frac{1}{d^{i-\alpha}}$$

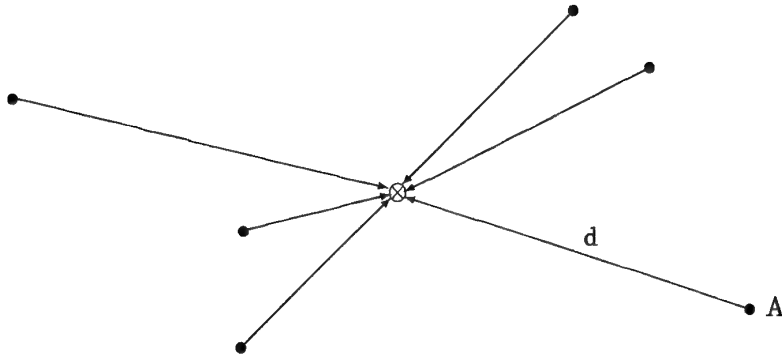where $i = 2$ or 3, depending on the source-receiver path medium.

Hence α gives the power-law exponent used for the particular propagation medium. Also, the value of α depends upon the source density. However, it is not clear how the source domain is determined.

N_I and A_α are scaling parameters, required in joining the two regions to form a smooth composite pdf. As such, they convey no physical meaning. Decreasing the N_I value will raise the region I $Eo/Erms$ value without affecting the exceedance probability value. Increasing the A_α value will also increase the Region I $Eo/Erms$ value, but will affect the exceedance probability value.

---

[3]A parameter with two subscripts indicates relevance to both Class A and B models.

(a) Multiple low-level sources. Envelope ≈ Rayleigh-distributed.

(b) Few (<10) high-level sources. Envelope ≈ Middleton-distributed.

Figure 2: Source-receiver geometry. •-sources, ⊗-receiver.

For some idea of how the parameters affect the shape of the model on the RPP, refer to [5, Figures 2.1–2.4, 3.1, and 3.2] and especially [4, pages 91–99][4].

3   Parameter Estimation

The parameters are estimated according to their graphical significance by Middleton's method [6, especially pages 197–201]. For example, $\Phi_{A,B}$ is simply found by noting the $Eo/Erms$ value where the data departs from Rayleigh behaviour. This is relatively straight-forward, as are the methods of finding the other key parameters. Note that al-

---

[4]A more comprehensive study of the effects of parameter variation is given in the authors' notes on the subject.

though visually it may be easy to estimate the parameters, the algorithm's automated processes need to eliminate all subjectivity involved in such a method, which can become a problem with some of the more unusual data samples.

Parameter estimation for Class A is quite easy, as there are only three parameters. Φ_A is estimated by the method mentioned above; A_A by finding the inflection point. Ω_A is then scaled until the model and data appear more closely matched on the APD.

Class B parameter estimation can become difficult at times because of its complexity (six parameters). Φ_B and A_B are found by a similar method as above, however the remaining parameters introduce difficulty. α and Ω_B are given an arbitrary (but sensible; in the middle of their allowable ranges) value as a starting point. These four parameters describe Region II, so they are passed into an optimisation routine specifically for this region. Once these four parameters are found it becomes necessary to estimate the values of N_I and A_α that will result in a smooth composite function around the inflection point. This is done by forcing two requirements upon the model:

(1) $\frac{dP_{BI}}{d\epsilon_0} = \frac{dP_{BII}}{d\epsilon_0}$ in the Rayleigh region.

(2) $P_{BI} = P_{BII}$ at the inflection point.

Requirement (1) states that in the straight-line Rayleigh section of the RPP, the two regions must have the same gradient, and requirement (2) stipulates that the two regions must have the same value at the *composite function's* inflection point. Applying the above arguments to Equations 1 and 2, it can be shown that:

$$A_\alpha = \frac{e^{-A_B} \times \beta_3 \times \Gamma(1 - \alpha/2) \times \epsilon_B^\alpha}{4 \times G_B^2 \times \Gamma(1 + \alpha/2)(1 + \epsilon_B^{-\alpha})} \times \left(\frac{e^{-A_B} \times \beta_2 - 1}{\beta_1}\right)^{\alpha/2}, \tag{4}$$

where:

$$\beta_1 = \sum_{n=0}^{\infty} \frac{(-1)^n \hat{A}_\alpha{}^n \Gamma(1 + \alpha n/2)}{n!},$$

$$\beta_2 = \sum_{m=0}^{\infty} \frac{A_B^m \times (\sigma_B)^{-1}}{m!},$$

$$\text{and } \beta_3 = \sum_{m=0}^{\infty} \frac{A_B^m \times \text{Exp}[\frac{-\epsilon_B^2}{\sigma_B}]}{m!},$$

$$\text{where } \epsilon_B \equiv \text{ inflection point}$$

with $\hat{A}_\alpha$ as in Equation 1, and σ_B as in Equation 2.

A_α is found by solving for the root of Equation 4. This form cannot be solved algebraically, so an iterative procedure was written to find the numerical value. Once the value of A_α is found, N_I may be found easily by use of the following equation derived from requirement (1);

$$N_I = \frac{e^{-A_B} \times \beta_2 - 1}{\beta_1} \tag{5}$$

This completes the parameter estimation and allows the formulation of a smooth composite function. However, the above method for estimating A_α and N_I is not accurate enough; another optimisation routine is needed to optimise these two parameters, using the remaining four parameters to implement the Region I part of the model.

The above procedure is one suggested method for parameter estimation. Others exist, some estimating on a sample-by-sample basis [16].

4   Model Implementation

The model is implemented by various routines using the "Mathematica" software package. The routines perform the following: (i) estimation of the parameters, (ii) modelling of the data, (iii) a (limited) optimisation of the parameters, and (iv) characterisation of the data sets. The most crucial step is selecting the inflection point. Knowledge of this allows a graphical categorisation of the APD as Class A or B; a large gradient at the inflection point implying Class A, while a smaller gradient implying Class B. In reality, both models are fitted to the data because of a number of borderline cases: it becomes difficult to label some either way. Class B models are orders of magnitude slower to evaluate than Class A because of the need to evaluate Gamma and Hypergeometric functions.

The routines test the validity of the model with respect to the data sets. This involves a 95% significance level Kolmogorov-Smirnoff (K-S) goodness-of-fit test [2], which is recommended by Middleton [7, page 214.] Other procedures test whether either model will be valid under all circumstances, by (amongst others) testing the angle of the inflection point[5].

5   Parameter Optimisation

Optimisation (for our purposes) is the minimisation of the sum of the squares of the errors between the dataset APD and the model APD. Hence optimisation of the model parameters shapes the model APD in order to minimise this statistic.

Fortran 77 programs are used to perform the optimisation using quasi-Newton and finite-difference gradient methods [10]. These programs operate at much faster rates than those written in Mathematica, with the disadvantage that several numerical evaluation

---

[5] A good measure of whether a Class B model will fit a data set is the maximum (transformed) difference of the exceedance probabilities between the data and an optimised Class A model. If it is above a certain threshold, a Class B model will not be possible, and hence one or more assumptions are erroneous.

problems present themselves[6].

The optimisation of Class A model parameters is quite straight forward and does not require special optimisation software. Region II of the Class B model, although having an extra parameter α, behaves in exactly the same way as a Class A model. The extra parameter still allows simple and predictable adjustment of the APD in this Region.

The principle difficulty lies in optimising Region I of the Class B model. The shape and scale effects of the four parameters here are not well understood or predictable, and specially-written optimisation software must be used. It was found that the initial estimates of the parameters need to be carefully selected for the optimisation to converge correctly. Haphazard selection of the estimates may lead to an optimisation routine converging to a local (rather than global) minimum.

Upon optimising the model, the implementation of the figure of merit for the goodness of fit should be thought of carefully. The K-S test is insensitive to rare-event discrepancies (difference between data and model) the less 'rare' they become. The rare events are important in the process, because of the need to include impulsive behaviour in the models, and hence a K-S test on the whole exceedance probability range is inappropriate. What is needed is a statistical test that weights increasingly smaller probabilities more heavily. The Anderson-Darling statistic has this property and may be effective [15, Sec. VIII].

6   Data Acquisition

Data acquisition is a vital step before the modelling process, and issues such as sampling rates and stationarity must be addressed and resolved before modelling takes place.

Ideally, the sampling rate should be above the Nyquist rate (twice the highest frequency component) to avoid aliasing [11, 1.4.1 and 1.4.2]. Remembering that the Class B model is a model of band-limited EMI anyway, it becomes apparent that this does not pose a problem. However, the sampling (and hence filtering) should be performed such that the high-frequency impulsive nature of the EMI is not drastically altered. As is shown elsewhere [12, pp. 44,45], excessively narrow filter bandwidths cause attenuation of rare events (say those around 0.0001% exceedance probability on the APD) by as much as 20

---

[6]Primarily, the problem is the implementation of Kummer's Confluent Hypergeometric function from first principles. Various solutions are given in text [9], however the authors have derived a recursive equation, shown below, that eliminates several numerical evaluation problems:

$$M(a, b, z) = \sum_{n=0}^{\infty} M_n,$$

where:

$$M_n = \begin{cases} 1 & \text{if } n = 0 \\ \frac{az}{b} & \text{if } n = 1 \\ \frac{(a+n-1)z}{(b+n-1)n} M_{n-1} & \text{if } n > 1 \end{cases}$$

dB by changing the bandwidth by only several kHz. A change of this magnitude may well render a Middleton model ineffective. The attenuation will take the form of high, narrow power peaks being amplitude-clipped and pulse-width extended. Hence persistence of 'flat' APD's of apparently Class B form may be caused by low sampling rates.

It was suspected that autocorrelation caused by oversampling would affect the probability values on the APD. To study the effects of autocorrelation, every n^{th} value was taken, where n ranged from 2 to 10. It was found that the effects were negligible: taking the nth sample did not appreciably alter the APD below around $n = 10$, and hence it was assumed autocorrelation did not pose a problem in the analysis.

It is important to have stationary data for the modelling process, as it is one of the assumptions Middleton makes. Nonstationarity becomes more of a problem the longer the data acquisition period is, however, this (it would seem excessive) time is needed to establish the 'rare event' portion of the sample set. This is because with large (but finite) sample sets, even in the order of hundreds of millions of samples, the 'rare events' portion of the model will not necessarily represent the respective portion of the EMI closely. There may in the order of ten or less samples representing the data in these portions[7]. It would seem that a compromise must be reached in this process: dividing the data into smaller intervals giving different APD's implies nonstationarity of the whole interval, but one can only divide so far, as APD's can only accurately represent the data when they are above a certain sample size.

Specific examples of modelling may be seen in another report [1]. This report shows in more detail the practical problems associated with modelling and simulation.

7 Conclusions and Recommendations

The procedures outlined in this paper provide the basis for an elementary analysis of the APD's of EMI. Middleton's papers alone may not do so. The bulk of his papers give intricate details as to the mathematics of devising the various models: they do not give a good foundation for a practical utilisation of the models, nor do they approach the problems associated with such a task. As Middleton's papers are both repetitious and confusing, the authors have attempted to explain the models in simpler terms, disregarding most theory and focusing on explanation and implementation.

The Middleton model approach offers substantial advantages over other analysis and characterisation methods; the primary one being the physical nature of the models. With a good understanding of the theory and implementation, Middleton modelling may prove to be a valuable tool.

---

[7]For example, sampling at 10 kHz for 10 minutes will produce an APD with the rare events portion (say 0.0001%) being represented by (on average) only 6 samples.

References

1. M. S. Britton, M. L. Scholz, *Modelling Hf EMI Using Middleton Models: Results of Trials and Procedures for Simulation*, Defence Science and Technology Organisation Technical Report DSTO–TR–0235, August 1995.

2. J. D. Gibbons, S. Chakraborti, *Nonparametric Statistical Inference*, 3rd ed., 1992.

3. D. Middleton, *Statistical-Physical Models of Man-Made Radio Noise-Part I: First-Order Probability Models of the Instantaneous Amplitude*, U.S. Department of Commerce OT Report 74–36, April 1974.

4. D. Middleton, *Statistical-Physical Models of Man-Made Radio Noise-Part II: First-Order Probability Models of the Envelope and Phase*, U.S. Department of Commerce OT Report 76–86, April 1976

5. D. Middleton, *Statistical-Physical Models of Electromagnetic Interference*, IEEE Trans. Electromagn. Compat., Vol EMC-19, No.3, pp.106–127, August 1977.

6. D. Middleton, *Procedures for Determining the Parameters of the First-Order Canonical Models of Class A and Class B Electromagnetic Interference*, IEEE Trans. Electromagn. Compat., Vol EMC-21, No.3, pp.190–208, August 1979.

7. D. Middleton, *Canonical Non-Gaussian Noise Models: Their Implications for Measurement and for Prediction of Receiver Performance*, IEEE Trans. Electromagn. Compat., Vol EMC-21, No.3, pp.209–220, August 1979.

8. D. Middleton, *Multi-Dimensional Detection and Extraction of Signals in Random Media*, Proc. IEEE 58, No. 5, pp. 696–706.

9. M. Abramowitz, I. A. Stegun, *Handbook of Mathematical Functions*, 8th ed., 1972.

10. *IMSL Library of Fortran Routines for Mathematical Applications*.

11. J. G. Proakis, *Digital Signal Processing: Principles, Algorithms, and Applications*, 2nd ed., 1992.

12. E. N. Skomal, *Man-Made Radio Noise*, 1978.

13. V. V. Kabanov, *Model of the Amplitude Probability Distribution of Atmospheric Radio Noise*, Scipta Technica, pp 122–129, 1988.

14. E. Jakeman, R. J. A. Tough, *Non-Gaussian Models for the Statistics of Scattered Waves*, Advances in Physics, Vol. 32, No. 5, 471–529, 1988.

15. E. S. Pearson, H. O. Hartley, *Biometrika Tables for Statisticians: Volume II*, Biometrika Trust 1976.

16. S. M. Zabin, H. V. Poor, *Recursive Algorithms for Identification of Impulsive Noise Channels*, IEEE Trans. Information Theory, Vol. 36, No. 3, May 1990.

THIS PAGE IS INTENTIONALLY BLANK

Distribution

DEPARTMENT OF DEFENCE

Defence Science and Technology Organisation

Chief Defence Scientist	1
DSTO Central Office Executive members	
Counsellor, Defence Science, London	Doc Cntl Sht
Counsellor, Defence Science, Washington	Doc Cntl Sht
Scientific Adviser, POLCOM	1
Senior Defence Scientific Adviser	1
Assistant Secretary, Scientific Analysis	1
Director, Aeronautical and Maritime Research Laboratory	1

Electronics and Surveillance Research Laboratory

Chief, Communications Division	1
Chief, Information Technology Division	1
Research Leader, Military Information Networks	1
Research Leader, Secure Communications	1
Research Leader, Command, Control, Communications	1
Research Leader, Military Computing Systems	1
Research Leader, Command, Control and Intelligence Systems	1
Head, Network Architectures	1
M. S. Britton	1
M. L. Scholz	1

Navy Office

Navy Scientific Adviser (NSA)   1

Army Office

Scientific Adviser, Army (SA-A)   1

Air Office

Air Force Scientific Adviser (AFSA)   1

Library and Information Services

Defence Central Library, Technical Reports Centre	1
Manager, Document Exchange Centre	1
DSTO Salisbury Research Library	2
Library, Defence Signals Directorate, Canberra	1

Headquarters Australian Defence Force

Development Division

Director General, Force Development (Joint)	1
Director General, Force Development (Land)	1
Director General, Force Development (Air)	1
Director General, Force Development (Sea)	1
Director Communications Development	1
Director Communications and Info. System Policies and Plans	1

Operations Division

Director General, Joint Communications and Electronics	1

Acquisition and Logistics Program

Defence Materiel Division

Director General, Joint Projects Management Branch	1
Assistant Secretary, Comms. and Info. Systems Eng. Branch	1
Director, Communications Engineering Development	1

Strategy and Intelligence Program

Force Development and Analysis Program

Assistant Secretary, Project Development	1

Defence Intelligence Organisation

Deputy Director, Defence Intelligence Organisation	1

Defence Signals Directorate

Director, Defence Signals Directorate	1

Spares

DSTO Salisbury Research Library	6

Department of Defence

DOCUMENT CONTROL DATA SHEET

3a. AR Number AR-009-365	3b. DSTO Number DSTO-TR-0234	3c. Type of Report TECHNICAL REPORT	4. Task Number ADF93/319	
5. Document Date August 1995	6. Cost Code 837795	7. Security Classification	8. No of Pages	11

10. Title

A PRACTICAL UTILISATION OF MIDDLETON MODELS: AUTOMATED MODELLING, PARAMETER ESTIMATION AND OPTIMISATION.

7. Security Classification

* | U | U | U |

Document   Title   Abstract

S (Secret) C (Confi) R (Rest) U (Unclassified)

* For UNCLASSIFIED docs. with a secondary distribution LIMITATION, use (L) in document box.

| 9. No of Refs | 16 |

11. Author(s)

M. S. BRITTON

12. Downgrading/Delimiting Instructions
NONE NECESSARY IN FUTURE

13a. Corporate Author and Address

M. L. SCHOLZ
COMMS DIV., NA DISCIPLINE
BLDG 34, TSAS

13b. Task Sponsor

DGFD(J)

14. Officer/Position responsible for

Security: SOESRL

Downgrading: N/A

Approval for Release: NEIL BRYANS (CCD)

15. Secondary Release Statement of this Document

APPROVED FOR PUBLIC RELEASE

16a. Deliberate Announcement

No limitation

16b. Casual Announcement (for citation in other documents)

  ✔ No Limitation   ☐ Ref. by Author, Doc No. and date only

17. DEFTEST Descriptors

Electromagnetic Interference Modelling.

18. DISCAT Subject Codes

19. Abstract

A procedure is proposed for analysing electromagnetic interference (EMI) with Middleton models. An introduction to the models is given, and descriptions of automated procedures for estimation and optimisation of model parameters are proposed. Various techniques are developed to solve numerical problems in the calculation of the model parameters. Many of the practical problems associated in the analysis are outlined.